FIRST ANALYSIS OF THE ν_5 BAND OF DNO_3 (DEUTERATED NITRIC ACID) IN THE 11 μm REGION

J. Koubek[1,2], A. Perrin[2], H. Beckers[3], H. Willner[3]

[1]Institute of Chemical Technology, Department of Analytical Chemistry, Technická 5, 166 28, Prague, CZECH REPUBLIC

[2]Laboratoire Inter-universitaire des Systèmes Atmosphériques, CNRS, Université Paris 12, 61 Av. du Général de Gaulle, 94010 Créteil Cedex, FRANCE

[3]Anorg. Chemistry, University of Wuppertal, D-42119 Wuppertal, GERMANY

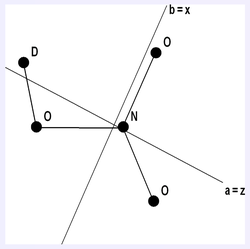

1 Introduction

Nitric acid (HNO_3) plays an important role as a "reservoir" molecule for both the NO_x (nitrogen oxides) and HO_x (hydrogen oxides) species in the stratosphere [1]. These radicals are potentially active contributors to the ozone destruction in the stratosphere through catalytic reactions. For this reason, various isotopic species of nitric acid have been the subject of numerous spectroscopic studies [2,3]. High resolution studies on nitric acid isotopomers in the infrared, submillimeter and centimeter region are referred in the article by Drouin *et al.* [4] DNO_3 isotopomer is referred particularly by Chou *et al.* [5]

In the infrared, just the ν_9 (O–D torsion) [6] , ν_8 (out of plane NO_2 bend) [7] , ν_7 (O–NO_2 bend) [8] , ν_6 (O–NO_2 stretch) [8] and ν_2 (NO_2 a-stretch) [9] fundamental bands were subjects of high resolution FTIR studies by Tan, Looi, Lua, Maki, Johns and Noël. The present analysis describes the first analysis of the ν_5 (NO_2 planar bend) band of DNO_3 in the 11 μm spectral region.

2 Experimental

DNO_3 was synthesized from D_2SO_4 and KNO_3 by using vacuum techniques in Wuppertal. The sample contained traces of HNO_3, H_2O, HDO, D_2O, NO_2 - these impurities served in calibration of the spectra using HITRAN database. The infrared spectrum of deuterated nitric acid was recorded on the Bruker IFS 120 HR Fourier transform spectrometer of Wuppertal in the 700–1500 cm^{-1} region at three pressures: 1 Torr, 0.3 Torr and less then 0.1 Torr (cf Figure 1). The instrumental resolution is 0.0022 cm^{-1} and the maximal spectral resolution is 0.0027 cm^{-1} (from minimal observed spacing between two lines that is greater than the FWHM of either line).

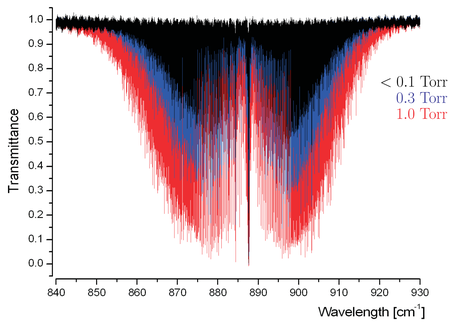

Figure 1: ν_5 band of DNO_3, spectrum measured in Wuppertal

3 Theory

DNO_3 is planar asymmetric molecule (C_S symmetry). The form of the Hamiltonian matrix used for DNO_3 is described in Table 1. The rotational operators for both the $v = 5^1$ and $v = 7^1 9^1$ vibrational diagonal blocks include Watson-type operators written in an I^r representation with an A-type reduction. Due to symmetry considerations, A-type and B-type Coriolis resonances are to be considered in the $5^1 \Leftrightarrow 7^1 9^1$ off-diagonal vibrational operators. The resonance between the 5^1 and $7^1 9^1$ levels is indeed very strong.

Table 1: Hamiltonian matrix

	5^1	$7^1 9^1$
5^1	$H_{5,5}$	complex conjugate
$7^1 9^1$	$H_{79,5} = C_A + C_B$	$H_{79,79}$

v-diagonal operator (rotational operator):

$H_{v,v} = E_v + A_v J_z^2 + B_v J_x^2 + C_v J_y^2 + \Delta_K^v J_z^4 - \Delta_{JK}^v J^2 J_z^2 - \Delta_J^v (J^2)^2 - 2\delta_J^v J^2 J_{xy}^2 - \delta_K^v \{J_z^2, J_{xy}^2\} + \ldots$

v-off-diagonal operators: $H_{79,5} = C_A + C_B$:

$C_A = C_{A1} J_z + C_{A2} \{iJ_y, J_x\}$

$C_B = C_{B1} J_x + C_{B2} \{iJ_y, J_z\} + C_{B3} J_x J^2 + C_{B4} J_x J_z^2 + C_{B5} (J_+^3 + J_-^3)$

$\{A, B\} = AB + BA; J_{xy}^2 = J_x^2 - J_y^2; J_\pm = J_x \pm iJ_y$

Due to the close proximity of the 5^1 and $7^1 9^1$ energy levels of 14–DNO_3, strong perturbations are observed in the spectrum. Due to the relative symmetry of the $5^1 \Leftrightarrow 7^1 9^1$ interacting states ($A' \Leftrightarrow A''$), A-type and B-type Coriolis resonances are to be considered for the energy levels calculation. Through these interactions, the $7^1 9^1$ "*dark*" *state* is populated on behalf of the 5^1 state. Thanks to this *line mixing*, many $\nu_7 + \nu_9$ transitions become *observable*.

This differs completely from the scheme of resonance observed for 14–HNO_3 and 15–HNO_3, since Fermi and C-type Coriolis resonances are coupling the $5^1 \Leftrightarrow 9^2$ ($A' \Leftrightarrow A'$) resonating states.

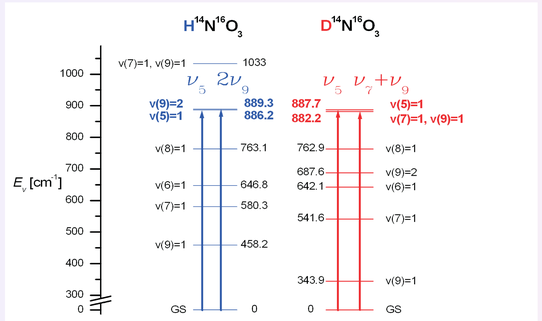

Figure 2: Energy level ladder for HNO_3 and DNO_3

4 Analysis of the $D^{14}N^{16}O_3$ infrared spectra

4.1 Assignment

3000 rovibrational transitions, approximately, of ν_5 band and cca 300 rovibrational transitions of $\nu_7+\nu_9$ were assigned using ground state combination differences with rotational ground state parameters achieved by Drouin *et al.* [4]. Least squares fit of molecular parameters enabled to synthesize satisfactorily the spectrum. Following figures demonstrate sufficient conformity between observed and calculated spectrum.

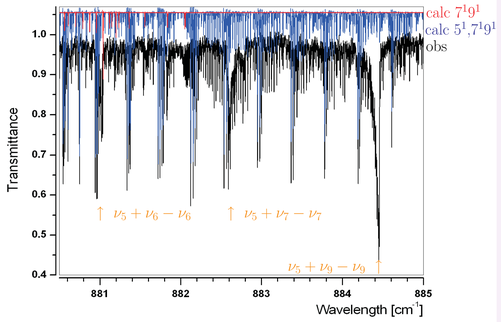

Figure 3: Hotbands' region

Figure 3 shows the region where three hot bands occur: $\nu_5+\nu_6-\nu_6$, $\nu_5+\nu_7-\nu_7$ and $\nu_5+\nu_9-\nu_9$ located at cca 881, 883 and 884 cm^{-1}, respectively. These bands were not considered in the analysis.

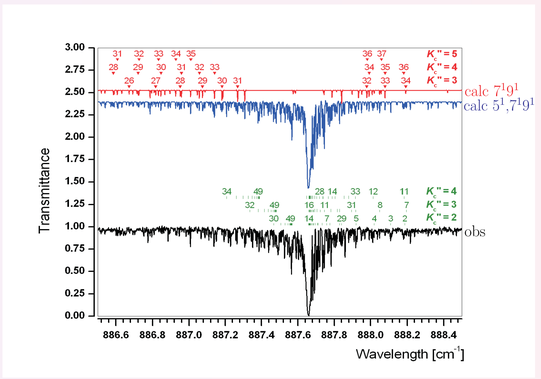

Figure 4: ν_5 Q branch region

Figure 4 shows the ν_5 region of the very dense Q branch, severely mixed with $\nu_7 + \nu_9$ transitions. Several $J(K_c'')$ packets of ν_5 transitions (green colour labels) and $\nu_7 + \nu_9$ transitions (red colour labels) are sorted with following selection for upper and lower states: $J\ K_a' = J - K_c'\ K_c' \longleftarrow J\ K_a''\ K_c''$.

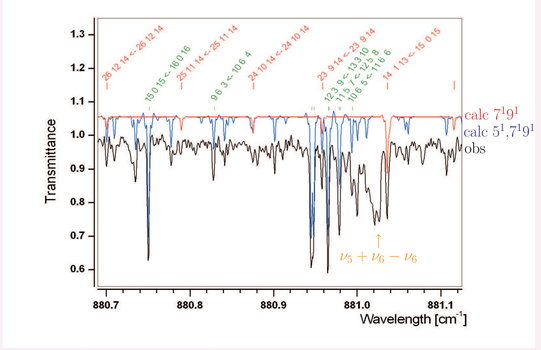

Figure 5: Hotbands' region - detail

Figures 5 and 6 show detailed part of the spectrum. In Figure 5, P lines and Q lines belonging to the ν_5 band together with lines from the resonating $\nu_7+\nu_9$ dark bands are evidenced. Figure 6 shows the central part of the ν_5 Q branch.

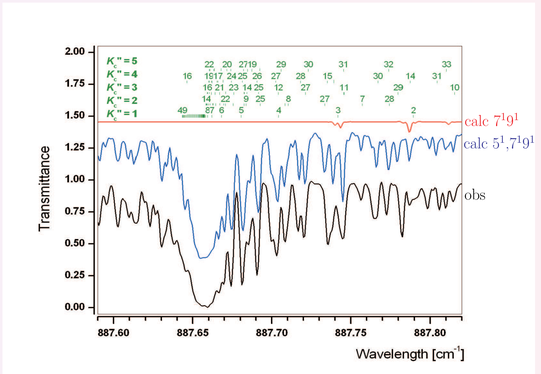

Figure 6: ν_5 Q branch central region

4.2 Fit

Line positions and intensities were determined from least squares fit on a rather large set of experimental data as shows Table 2. All values of parameters are in cm^{-1}, the uncertainty in the last digits (one standard deviation) is given in the parenthesis.

Table 2: Molecular rovibrational parameters

Parameter	5^1	$7^1 9^1$
E_v	887.657124(81)	882.21072(49)
A	0.43244023(96)	0.4317699(37)
B	0.3765583(20)	0.3757854(37)
C	0.20048282(20)	0.2001817(30)
Δ_K	$1.629(46)\times10^{-7}$	$2.85(12)\times10^{-7}$
Δ_{JK}	$0.262(46)\times10^{-7}$	$-0.43(11)\times10^{-7}$
Δ_J	$2.1928(53)\times10^{-7}$	$2.258(17)\times10^{-7}$
δ_K	$3.478(17)\times10^{-7}$	$1.881(59)\times10^{-7}$
δ_J	$0.8929(28)\times10^{-7}$	$1.209(19)\times10^{-7}$
$5^1 \Leftrightarrow 7^1 9^1$ Coriolis interaction parameters		
Operator, Constant	Value	
J_z, C_{A1}	$3.4523(51)\times10^{-2}$	
$\{iJ_y, J_x\}$, C_{A2}	$3.997(12)\times10^{-4}$	
J_x, C_{B1}	$7.1521(68)\times10^{-2}$	
$\{iJ_y, J_z\}$, C_{B2}	$1.3064(22)\times10^{-3}$	
$J_x J^2$, C_{B3}	$-6.15(23)\times10^{-7}$	
$J_x J_z^2$, C_{B4}	$6.128(62)\times10^{-6}$	
$J_+^3 + J_-^3$, C_{B5}	$1.322(27)\times10^{-6}$	

The rms deviation of the fit with all weighted lines was about 0.51×10^{-3} cm^{-1}. Still, the assignment of some $\nu_7 + \nu_9$ transitions in the ν_5 Q branch is problematic.

Table 3: Statistics of the fit

fit of 1096 experimental energy levels (979 levels for ν_5 and 117 levels for $\nu_7+\nu_9$)				
0. 10^{-3}cm^{-1}	<	92.7 % of levels	<	1. 10^{-3}cm^{-1}
1. 10^{-3}cm^{-1}	<	4.6 % of levels	<	2. 10^{-3}cm^{-1}
2. 10^{-3}cm^{-1}	<	2.3 % of levels	<	4. 10^{-3}cm^{-1}
4. 10^{-3}cm^{-1}	<	0.4 % of levels	<	10. 10^{-3}cm^{-1}

Acknowledgements

The work of J.K. was supported through the Ministry of Education, Youth and Sports of the Czech Republic (research program LC06071) and a scholarship of the French government (Bourse du Gouvernement Français - Bourse de Doctorat en co-tutelle).

References

[1] World Meteorological Organization, *in* "Scientific Assessment of Ozone Depletion: 2006" (WMO, Ed.), Geneva, 2007.

[2] A. Goldman, C. P. Rinsland, A. Perrin, and J.-M. Flaud, *J. Quant. Spectrosc. Radiat. Transfer* **60,** 851–861 (1998).

[3] A. Perrin, *Spectrochim. Acta* **54,** 375–394 (1998).

[4] B. J. Drouin, C. E. Miller, J. L. Fry, D. T. Petkie, P. Helminger, and I. R. Medvedev, *J. Mol. Spectrosc.* **236,** 29–34 (2006).

[5] S. G. Chou, D. T. Petkie, R. A. H. Butler, and C. E. Miller, *J. Mol. Spectrosc.* **211,** 284–285 (2002).

[6] T. L. Tan, E. C. Looi, K. T. Lua, A. G. Maki, J. W. C. Johns, and M. Noël, *J. Mol. Spectrosc.* **150,** 486–492 (1993).

[7] T. L. Tan, E. C. Looi, K. T. Lua, A. G. Maki, J. W. C. Johns, and M. Noël, *J. Mol. Spectrosc.* **149,** 425–434 (1991).

[8] A. G. Maki, T. L. Tan, E. C. Looi, K. T. Lua, J. W. C. Johns, and M. Noel, *J. Mol. Spectrosc.* **157,** 248–253 (1993).

[9] T. L. Tan, E. C. Looi, K. T. Lua, A. G. Maki, J. W. C. Johns, and M. Noel, *J. Mol. Spectrosc.* **166,** 97–106 (1994).